Convex and Concave Surface Curvature Effects in Wall-Bounded Turbulent Flows

Marshall C. Richmond*
Battelle/Marine Sciences Laboratory, Sequim, Washington 98382
and
Virendra C. Patel†
University of Iowa, Iowa City, Iowa 52242

A fully ellipitic numerical method developed to solve the two-dimensional Reynolds-averaged Navier-Stokes equations for an incompressible fluid is employed in a computational study of several flows involving convex and concave surface curvature. The k-ϵ turbulence model and a variant of it, proposed to improve the calculation of flows with streamline curvature, are used in conjunction with a one-equation near-wall model. The performance of the method is examined through computations of fully developed curved duct flow and boundary layers on curved surfaces. In each case the main features of the flow are consistently reproduced. However, the computations tend to overpredict the convex wall skin friction and underpredict the concave wall skin friction.

Introduction

NUMEROUS experiments over the years have been conducted to study the influence of longitudinal surface curvature on wall turbulence in general and on turbulent boundary layers in particular. In most of these studies the experimental arrangements were such that there were streamwise pressure gradients, particularly at the junctions of flat and curved surfaces, although some investigators used special configurations to reduce or eliminate them. Nevertheless, experiments with longitudinal surface curvature invariably involve pressure gradients normal to the surface that are not accounted for in boundary-layer theory. In spite of this, most experiments have been conducted from the perspective of boundary-layer flows, in which the pressure field is assumed to be independent of the viscous flow.

Experimental investigations on the effects of surface curvature on turbulent boundary layers are exemplified by the works of Smits et al.[1] and Gillis and Johnston.[2] Both works were concerned with boundary layers developing on the walls of rectangular ducts in which an initially straight section was followed by a bend and another straight recovery section. Measurements were made in the boundary layer before, during, and after exposure to surface curvature. Smits et al. investigated the effects of short fetches of both convex and concave curvature, but strong streamwise pressure gradients were present at the bend inlet and exit on both walls. Gillis and Johnston, on the other hand, studied only the effects of convex curvature, but produced a nominally zero streamwise pressure gradient by modifying the tunnel geometry and flow along the outer, concave wall. These modifications were not documented, since they were not considered pertinent to the problem under investigation. In addition to the differences in streamwise pressure gradients, significant normal pressure gradients were present in both experiments. The results of the two experiments on the convex wall differ mainly in the recovery region downstream of the curvature. The data of Smits et al. indicate that the boundary layer had more or less returned to a typical flat-wall structure at the end of the recovery region, whereas those of Gillis and Johnston show that the boundary-layer structure, and especially the skin friction, were far from recovery at the last measurement station. There are many possible reasons for this discrepancy, including different lengths of exposure to curvature, effects of streamwise and normal pressure gradients, and secondary motions introduced by the duct bend.

The many computational studies pertaining to the effects of surface curvature have also tended to view the problem from the perspective of boundary-layer theory. Thus, solutions of boundary-layer equations, using different turbulence models and modifications thereof, have been compared with available data to ascertain the influence of curvature on the development of the boundary layer and turbulence structure, and to gauge the success with which these can be modeled. These studies have generally assumed that the pressure-gradient effects are well described by the equations and models and that, therefore, the residuary effects are due to curvature. The differences in the experimental results noted earlier are also reflected in the computations. For example, Gibson et al.[3] solved the boundary-layer equations with measured longitudinal pressure distributions and approximate normal pressure gradients, together with a Reynolds-stress turbulence model and wall functions, for both of the flows described above. For the case of Smits et al. the computed Reynolds stresses and skin-friction distributions agreed quite well with the data, but in the case of Gillis and Johnston rather poor agreement was obtained for the same quantities. These conflicting results illustrate that the underlying issues are far from resolved, insofar as the effects of surface curvature have not been isolated from those of pressure gradients, which always accompany practical configurations involving longitudinal surface curvature.

The principal aim of the present work was to carefully examine the effects of surface curvature and the attendant pressure gradients, both longitudinal and normal, through computations that, in principle, precisely account for these effects. In order to accomplish this it was necessary to abandon the boundary-layer methodology in which the pressure field is given and to approach the problem through solutions of the full Reynolds equations. It was necessary to also abandon turbulence models and solution procedures that rely on the wall-function approach, since, in a systematic study, it is essential to resolve the flow very close to the wall. Therefore, a robust numerical method was developed to solve the fully elliptic Reynolds equations for two-dimensional curved ducts (and ex-

Received Jan. 12, 1990; revision received June 12, 1990; accepted for publication July 5, 1990.

*Research Engineer, 439 West Sequim Bay Road. Member AIAA.
†Professor of Mechanical Engineering and Research Engineer, Iowa Institute of Hydraulic Engineering. Associate Fellow AIAA.

ternal flows) of quite arbitrary geometry, together with different treatments of the near-wall flow in the k-ϵ turbulence model, along the lines discussed by Chen and Patel.[4] Only an outline of the method is presented in the next section because it is described in detail by Richmond[5] along with numerous test cases in laminar and turbulent flows. This paper is concerned principally with the application of the method to a series of well-documented experimental flows in which pressure gradient and surface curvature effects are present.

We consider the case of fully developed turbulent flow in a long curved duct, for which experimental data were obtained by Eskinazi and Yeh,[6] to examine the effects of prolonged convex and concave surface curvatures with relatively mild pressure gradients. This is followed by two cases of developing boundary layers in curved ducts, one with a long fetch of curvature[7] and the other with a short fetch.[1]

Outline of the Calculation Method

The numerical method for two-dimensional flows utilized for this investigation incorporates several innovative computational techniques. The basic method is well developed and has been successfully applied to a wide variety of internal and external flow problems in addition to the cases considered here.

Numerical grid-generation methods are used to tranform the complex physical domain into a rectangular computational domain. The body-fitted coordinate system is generated by solving a system of Poisson equations with Neumann boundary conditions requiring the grid to be orthogonal on the boundaries of the domain. This latter feature facilitates the application of the boundary conditions, particularly at the wall in turbulent flows. The conservation equations of fluid motion are obtained by transforming the independent variables, namely, the coordinates, as well as the dependent variables, the velocity components. Such fully transformed equations are usually not employed in computational methods using body-fitted coordinates. However, with the velocity components aligned with the general nonorthogonal numerical coordinates, a staggered grid system can be used without difficulty even in highly curved geometries. The fully transformed equations for incompressible fluid motion have been derived using general tensor analysis and are presented in Richmond et al.[8] Among the equations listed there are continuity, Navier-Stokes, Reynolds-averaged Navier-Stokes, thermal energy, and transport of Reynolds stresses, turbulent kinetic energy, and the dissipation rate of turbulent kinetic energy.

For turbulent flows the Reynolds equations are closed using an isotropic eddy viscosity derived from the k-ϵ model with the generally accepted values of the five constants. In general, the near-wall flow can be treated using any of the approaches discussed by Chen and Patel.[4] For the present study the two-layer model they describe is used in all the calculations because of the need to account for the effects of adverse and favorable pressure graidents in zones of changing boundary curvature. Patel and Richmond[9] demonstrated both the importance of using near-wall models that can represent pressure gradient effects and the sensitivity of the wall shear stress to such modeling. In their study calculations of flat-plate boundary layers subjected to adverse and favorable pressure gradients showed that the two-layer model provides a more accurate and general description of pressure-gradient effects than do computations using simple wall functions. The two-layer model combines a one-equation model for the near-wall layer with the two-equation k-ϵ model for the fully turbulent outer layer. Using this scheme, the momentum, continuity, and turbulent kinetic energy equations are integrated to the wall, where the no-slip conditions are applied.

We also tested a variation of the standard k-ϵ model, proposed by Hanjalic and Launder, as outlined in Refs. 10 and 11 and hereafter referred to as the HL model. This model uses a different form of the generation term in the ϵ equation in an effort to provide a direct influence of streamline curvature on the length scale. This particualr model was chosen, over many others that claim to account for curvature effects, because the new form of the generation term is tensor invariant and does not require the introduction of additional model constants. The HL model was tested by Rodi and Scheuerer[11] for several curved shear layers with parabolic equations and was found to yield better results than those obtained with the standard k-ϵ model.

The transport equations of momentum and turbulence parameters are discretized using the so-called finite-analytic scheme developed by Chen.[12] In this method the convection-diffusion equations are linearized in each numerical element, solved analytically, and the solutions evaluated in terms of the unknown nodal values to obtain the algebraic representations at each grid point. The remainder of the solution procedure parallels that described in Patankar.[13] The calculations are perfomed on a staggered grid in the computational domain, and a modified version of the SIMPLER algorithm of Ref. 13, developed by Chen and Patel,[14] is used to determine the velocity field that satisfies the continuity equations and the corresponding pressure field. The pressure equation in this algorithm is solved using a number of downstream to upstream sweeps, usually 20, which significantly speeds up the convergence of the pressure field, especially for internal flows. The method employs a fully implicit time- and space-marching solution technique, although in the present study time plays the role of a global iteration step in the determination of a steady-state solution. The systems of algebraic equations are solved using a line-by-line method.

The method already outlined is stable and requires no smoothing or explicit under-relaxation other than that implied by variations in the time step. In principle, this method is capable of computing two-dimensional internal and external flows that are laminar or turbulent, separated or attached, steady or unsteady. Details of the equations, turbulence models, and numerical procedures are given in Richmond.[5]

Results and Discussion

Fully Developed Flow in a Curved Duct

The effects of prolonged convex and concave curvature on an initially fully developed straight-channel flow were studied by Eskinazi and Yeh.[6] The duct was strongly curved, having curvature ratios, defined as the ratio of the centerline radius of curvature to the duct width, of 11.5 and 9.5. The computational domain shown in Fig. 1 corresponds to the experimental geometry, with the following exceptions: The length of the upstream straight channel was taken to be 20 duct widths instead of the 64 in the experiments, and a straight section was

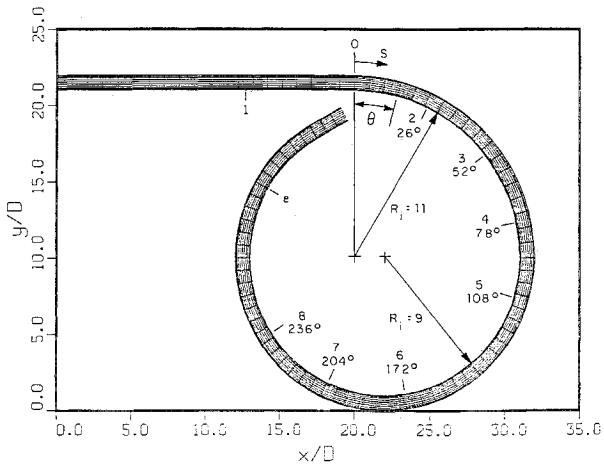

Fig. 1 Computational grid and measurement station numbers for the experiments of Eskinazi and Yeh.[6] S is the length along the inner or outer wall and R_i is the inner radius of curvature. Lengths are nondimensionalized by the duct width. Point e corresponds to the physical end of the wind tunnel.

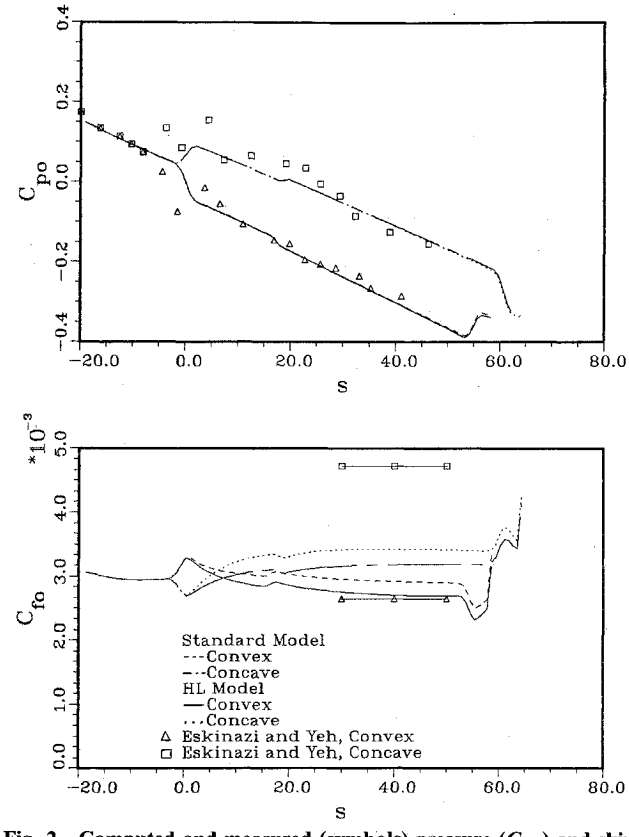

Fig. 2 Computed and measured (symbols) pressure (C_{p0}) and skin-friction (C_{f0}) coefficients for the experiments of Eskinazi and Yeh.[6]

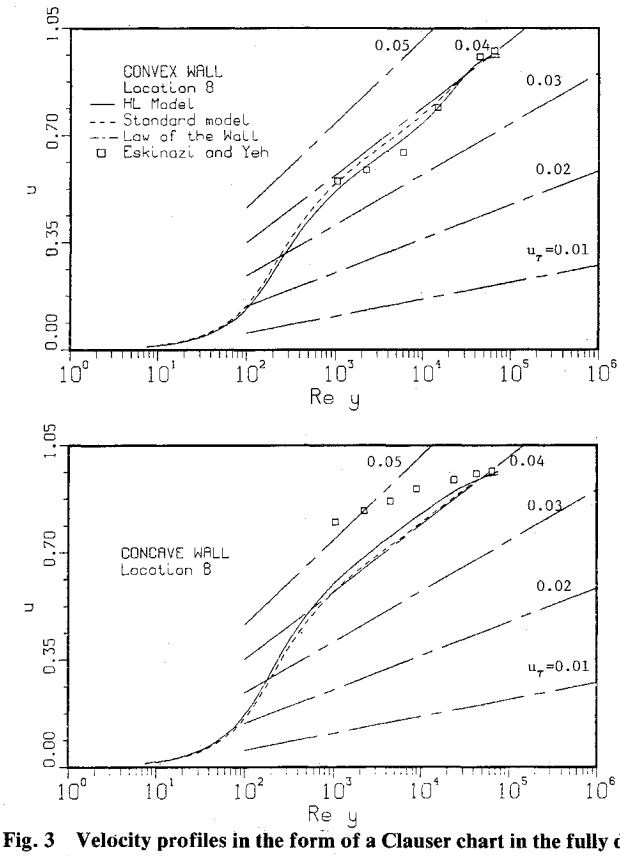

Fig. 3 Velocity profiles in the form of a Clauser chart in the fully developed region of the curved-duct flow.

added to the end of the wind tunnel, shown as point *e* in Fig. 1, to remove the influence of downstream boundary conditions. Note that the curved-duct section was constructed using two radii of curvature, thus allowing the duct to turn back on itself.

The calculations were performed on a grid, using 93 streamwise stations and 81 cross-stream nodes. The first grid point off the wall was located at $y^+ \sim 0.3$. The inner layer contained 26 grid points on both walls, and along the boundary between the inner and outer layers the turbulent Reynolds number remained in the neighborhood of 250. The computations were performed at the experimental Reynolds number of 148,400, which is based on the duct width and centerline velocity in the fully developed straight-channel flow. Values for the longitudinal and transverse velocity components (u,v) and turbulence parameters (k,ϵ) at the upstream boundary were specified using fully developed flow conditions based on a wall shear stress estimated from well-known straight-channel correlations. At the downstream boundary no conditions were specified for these variables becuase local parabolic flow was assumed. The pressure (p) was set to zero across this boundary, which is consistent with its location far from the end of the curve. The initial pressure field was simply assumed to be that which would exist in a fully developed straight-channel flow with length equal to the arc length along the duct centerline. The initial conditions for the other variables were obtained using a marching technique, as described in Ref. 5. The solution reached satisfactory convergence after 100 global iteration sweeps which required approximately 115 min of CPU time on a Prime 9950 minicomputer.

The grid dependency of the solution was examined by performing calculations on a coarser 50×53 grid. The only significant changes observed occurred in the pressure and wall shear stress distributions, which varied from the 93×81 grid results by less than 2%. The results presented subsequently were all obtained using the fine grid.

The pressure and skin-friction coefficients are shown in Fig. 2. Here, *s* is a dimensionless arc length measured along the inner (convex) or outer (concave) walls. The pressure at the start of curvature, $s=0$, on the convex wall was chosen as the reference pressure. The reference velocity is that used in the duct Reynolds number. No explanation for the large scatter in the experimental pressure distributions was given by Eskinazi and Yeh.[6] Nevertheless, the results obtained using the standard and HL models are in broad agreement with the data. Note that the small change in pressure near $s=20$ is due to the change in duct curvature. The sharp changes in the skin-friction near the end of the computational domain are due to the artificial extension of the duct geometry and downstream boundary conditions, but this has a negligible effect on the results in the fully developed region near $s=40$.

The wall shear stress is clearly affected by the steep pressure gradients near the changes in wall curvature as well as by the surface curvature itself. Beyond location 6, where $s \sim 30$, the flow again becomes fully developed. It is in this region that the skin friction predicted by the standard and HL models differs significantly. The HL model predictions are in agreement with the convex-wall data, but neither model is capable of predicting the high skin friction observed on the concave wall. The experimental wall shear stress was determined from the radial momentum equation. The experimental and calculated velocity profiles are plotted in the form of a Clauser chart in Fig. 3 to determine whether the profiles and skin friction are consistent with the law of the wall. On the convex wall this is indeed the case, but on the concave wall the velocity profile does not clearly show a logarithmic region. Presumably, a large portion of the differences between the measured and computed skin friction for the concave wall is due to local three-dimensional flow effects caused by the presence of Taylor-Goertler vortices. Although Eskinazi and Yeh did not report significant spanwise variations in their measurements, it seems reasonable to assume, based on other studies, e.g., Hunt and Joubert,[15] that the flow near the concave wall was affected by such vortices. The important contribution these vortices make to the concave wall flow is revealed by Moser and Moin[16] in a study of curved channel flow using direct turbulence simulation

techniques. Their calculations showed that Taylor-Goertler vortices accounted for nearly half of the difference between the convex and concave wall shear stress. Thus, two-dimensional computations, such as the present one, are unlikely to provide a complete and accurate description of the concave wall flow.

Figure 4 shows the velocity profiles across the channel at several of the measurement stations noted on Fig. 1. Note that the velocity is normalized by the measured or computed maximum velocity in each cross section. Upstream of the curve, the HL model and the standard k-ϵ model yield identical results, because in the absence of streamline curvature the dominant terms in the ϵ equation in each model are the same. In the curved section the HL model is an improvement over the standard model, especially for the concave wall flow. The level of improvement is similar to that obtained by Pourahmadi and Humphrey[17] using a complicated expression, given in cylindrical coordinates, for the proportionality constant in the eddy viscosity formula. The radial distributions of Reynolds shear stress ($-\overline{uv}$), turbulent kinetic energy (k), pressure difference (Δp), and eddy viscosity (ν_t) are shown in Fig. 5. Note the large changes in eddy viscosity required to bring about the relatively small improvement in the velocity profile of Fig. 4. This is a further indication that the concave wall flow is not two dimensional.

In general, the agreement between the computations and experiments is good, with the notable exception of the flow near the concave wall. A portion of the discrepancies can be attributed to three dimensionality in the flow, but the need for further refinement of the turbulence model to account for curvature effects is demonstrated by the performance of the HL model.

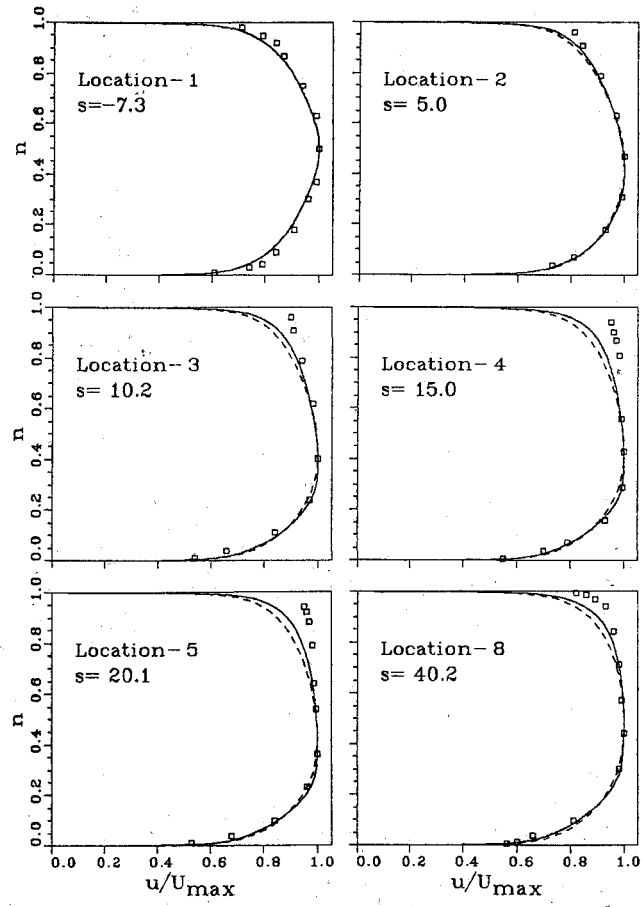

Fig. 4 Computed and measured (symbols) velocity profiles for the experiments of Eskinazi and Yeh:[6] U_{max} is the maximum velocity in the cross section, and n is the distance normal to the inner wall nondimensionalized by the duct width. Solid lines, HL model; dashed lines, standard k-ϵ model.

Boundary Layers on Curved Surfaces

Computations corresponding to the experiments conducted by Muck et al.,[7] Hoffmann et al.,[18] and Smits et al.[1] were performed. In these experiments measurements were made in boundary layers that were exposed to convex and concave curvature of varying length and severity. Muck et al. and Hoffmann et al. utilized the same wind-tunnel configuration, shown in Fig. 6, to study the effects of mild convex and concave curvatures, respectively. The geometry employed by Smits et al. is shown in Fig. 7. In both cases the end of the actual wind tunnel is located at the grid point e shown in Figs. 6 and 7. The ratios of the boundary-layer thickness to the radius of curvature, δ/R, for the studies considered here were $\delta/R \sim 0.01$ for Muck et al. and $\delta/R \sim 0.10$ for Smits et al. For the duct flow of Eskinazi and Yeh[6] considered earlier, the value of the half-width to radius ratio was approximately 0.06.

The numerical procedures employed for these cases were similar to those described for the fully developed flow calculations. Detailed results, e.g., velocity profiles, are presented for the convex and concave walls despite the significant and well-documented three-dimensional character of the concave wall flow in these experiments.

The geometry of Muck et al.[7] was described using a grid consisting of 97 streamwise stations and 81 cross-stream nodes. The computational domain utilized a shortened upstream section and a fictitious section added to the end of

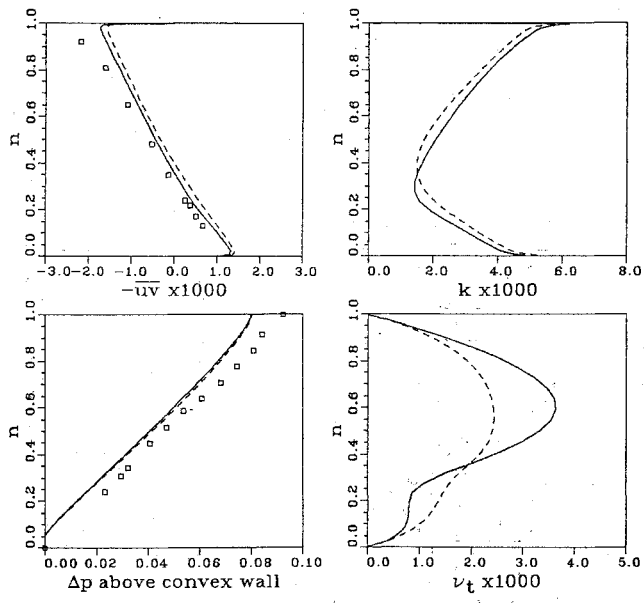

Fig. 5 Profiles of Reynolds shear stress ($-\overline{uv}$), turbulent kinetic energy (k), pressure (Δp), and eddy viscosity (ν_t) at station 8 of Eskinazi and Yeh.[6] Symbols are defined in Fig. 4.

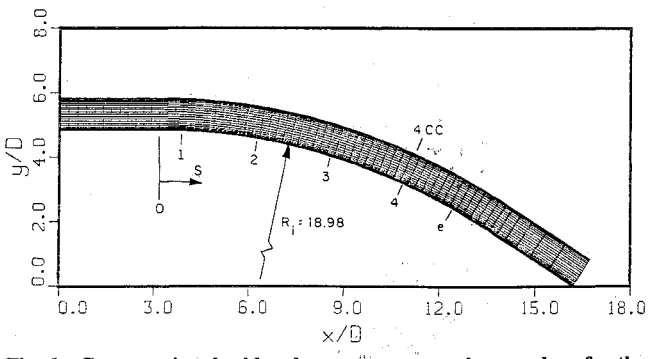

Fig. 6 Computational grid and measurement station numbers for the experiments of Muck et al.[7] (stations 1-4) and Hoffmann et al.[18] (station 4CC).

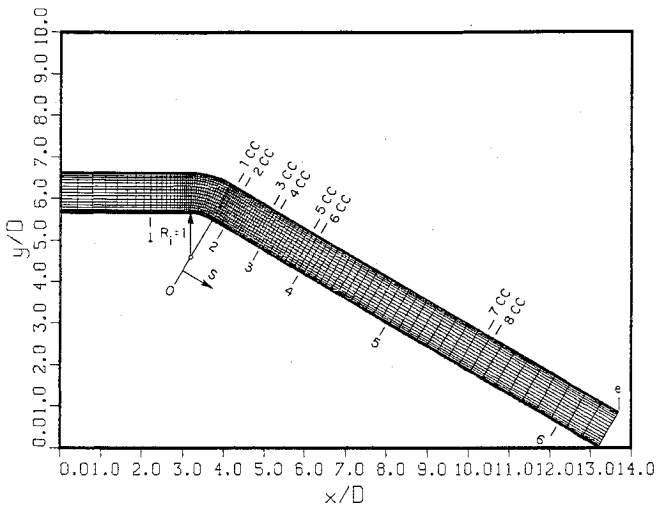

Fig. 7 Computational grid and measurement station numbers for the experiments of Smits et al.[1]

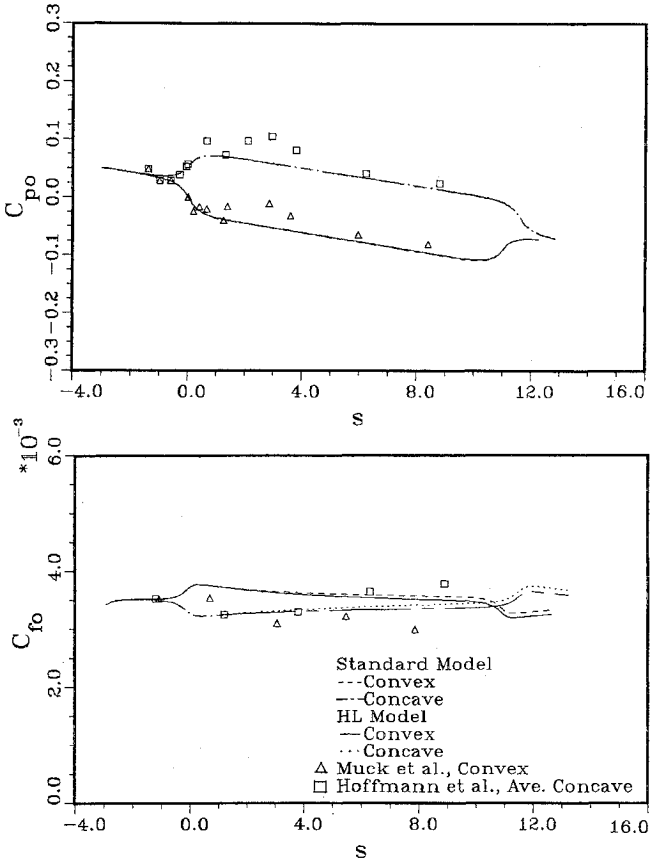

Fig. 8 Computed and measured (symbols) pressure (C_{p0}) and skin-friction (C_{f0}) coefficients for the experiments of Muck et al.[7] and Hoffmann et al.[18]

the wind tunnel for reasons previously explained. The pressure and skin-friction coefficients are shown in Fig. 8. Although unexplained variations in the experimental pressure distribution exist, the computed pressure follows the trend of the measurements. However, the computed skin friction does not agree well with the data, differing by as much as 20% for both the convex and concave walls. Since the curvature is relatively mild, the HL model produces only a slight improvement in the wall-friction coefficient. We note that a constant reference velocity has been used to define the skin-friction coefficient C_{f0}, so that Fig. 8 shows the actual variation of the wall shear stress. This definition avoids the uncertainties in defining a local freestream velocity in flows where normal pressure gradients are significant.

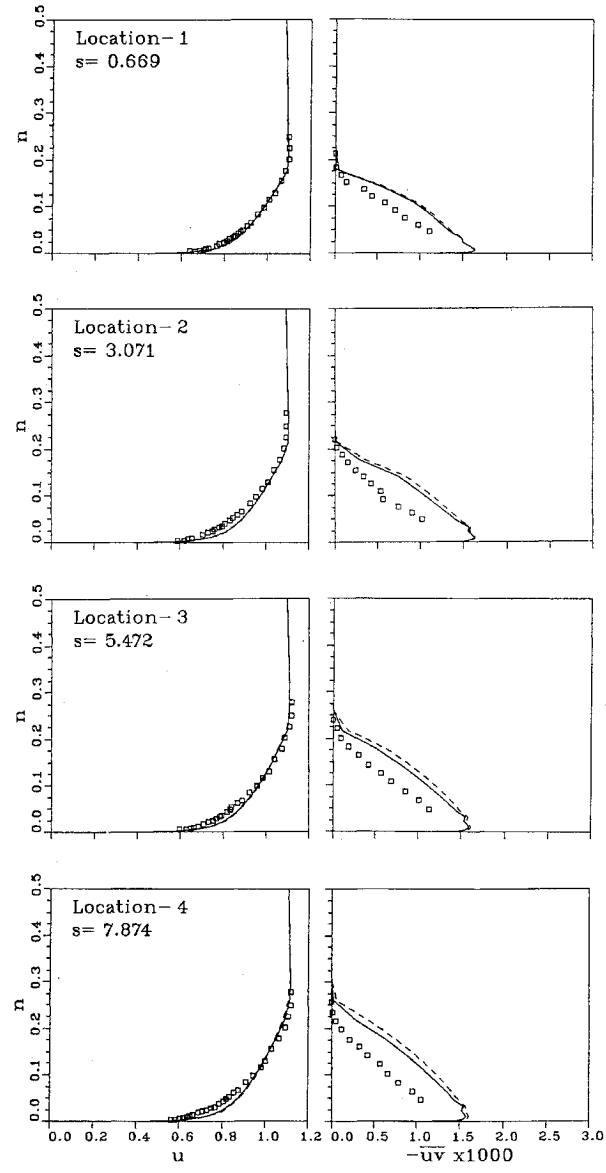

Fig. 9 Computed and measured (symbols) velocity and Reynolds shear stress profiles for the convex wall experiments of Muck et al.[7] The variable n is the distance normal to the convex wall nondimensionalized by the duct width. Solid lines, HL model; dashed lines, standard k-ϵ model.

Figure 9 shows the velocity and Reynolds stress profiles at several stations along the convex wall. The velocity profiles agree fairly well with the data, but the computed profiles are consistent with the overprediction of the wall shear stress. The Reynolds stress is overpredicted by both the standard and HL models. In this case the HL model is not particularly effective, because the large radius of curvature causes the HL model generation terms to be nearly the same as those of the standard model. It should be mentioned that these results are in accord with the boundary-layer calculations using the k-ϵ and algebraic stress models shown in the 1980–81 Stanford Conference[10] for the data of Hoffmann and Bradshaw,[19] which is a flow nearly identical to the one considered here.

Figure 10 compares the solution profiles at station 4CC (Fig. 6) on the concave wall with the measurements by Hoffmann et al.[18] The measurements shown in Fig. 10 correspond to the locations of spanwise maximum and minimum wall shear stress. At a point of maximum wall shear stress, the secondary flow induced by the longitudinal vortices forces fluid to move toward the wall, hence the increase in skin friction and decrease in the boundary-layer thickness at that loca-

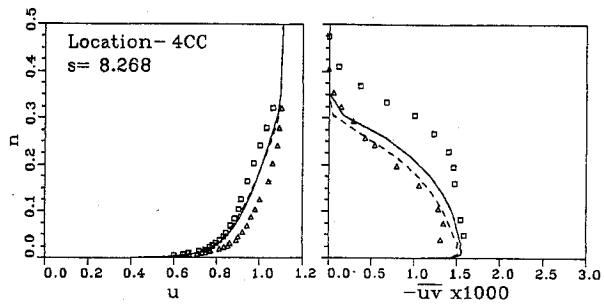

Fig. 10 Computed and measured (symbols) velocity and Reynolds shear stress profiles for the concave wall experiments of Hoffmann et al.[18] The variable n is the distance normal to the concave wall nondimensionalized by the duct width. Solid lines, HL model; dashed lines, standard k-ϵ model. Measurements at the point of minimum (squares) and maximum (triangles) wall shear stress.

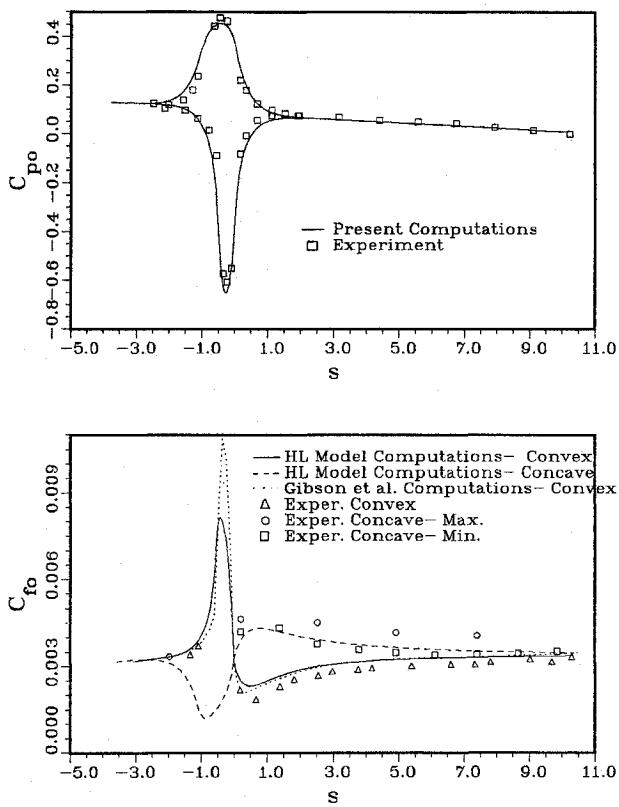

Fig. 11 Comparison of the computed pressure and skin-friction coefficients to the experiments of Smits et al.[1] and the computations of Gibson et al.[3]

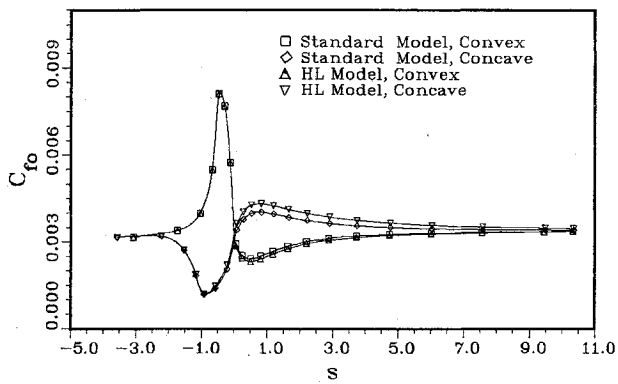

Fig. 12 Comparison of the skin-friction coefficients calculated using the standard k-ϵ and HL models.

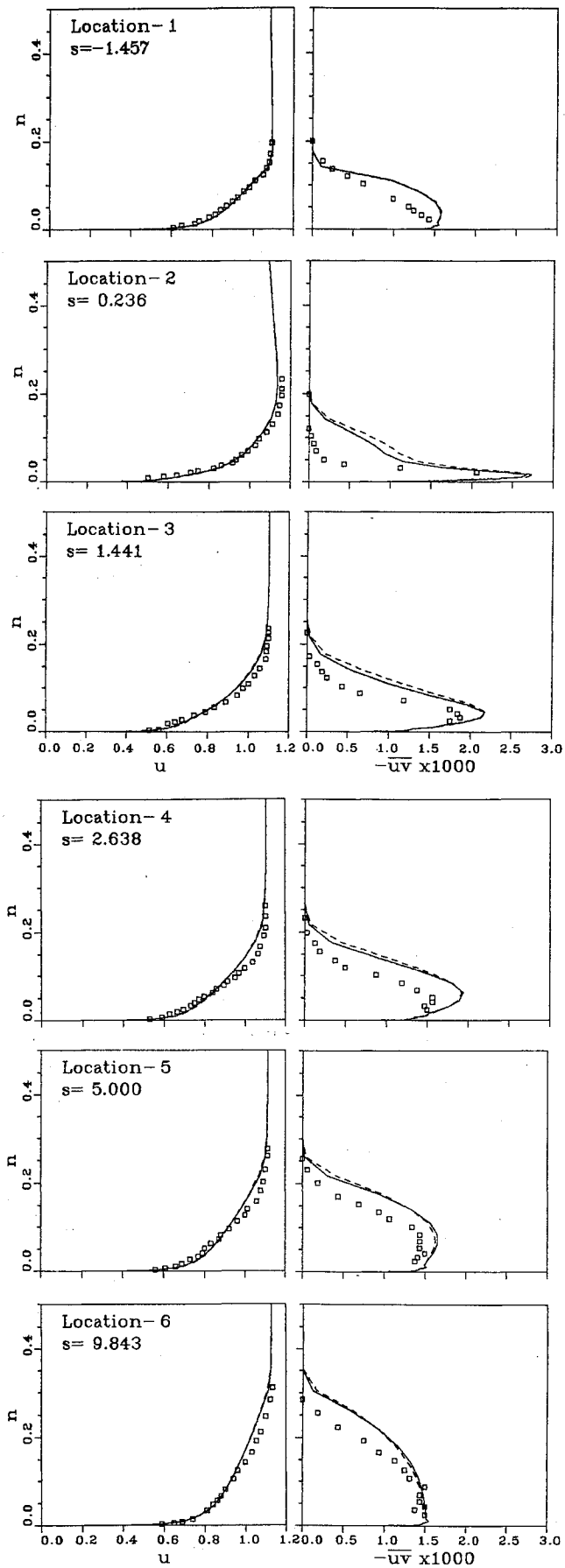

Fig. 13 Computed and measured (symbols) velocity and Reynolds shear stress profiles for the convex wall experiments of Smits et al.[1] The variable n is the distance normal to the convex wall nondimensionalized by the duct width. Solid lines, HL model; dashed lines, standard k-ϵ model.

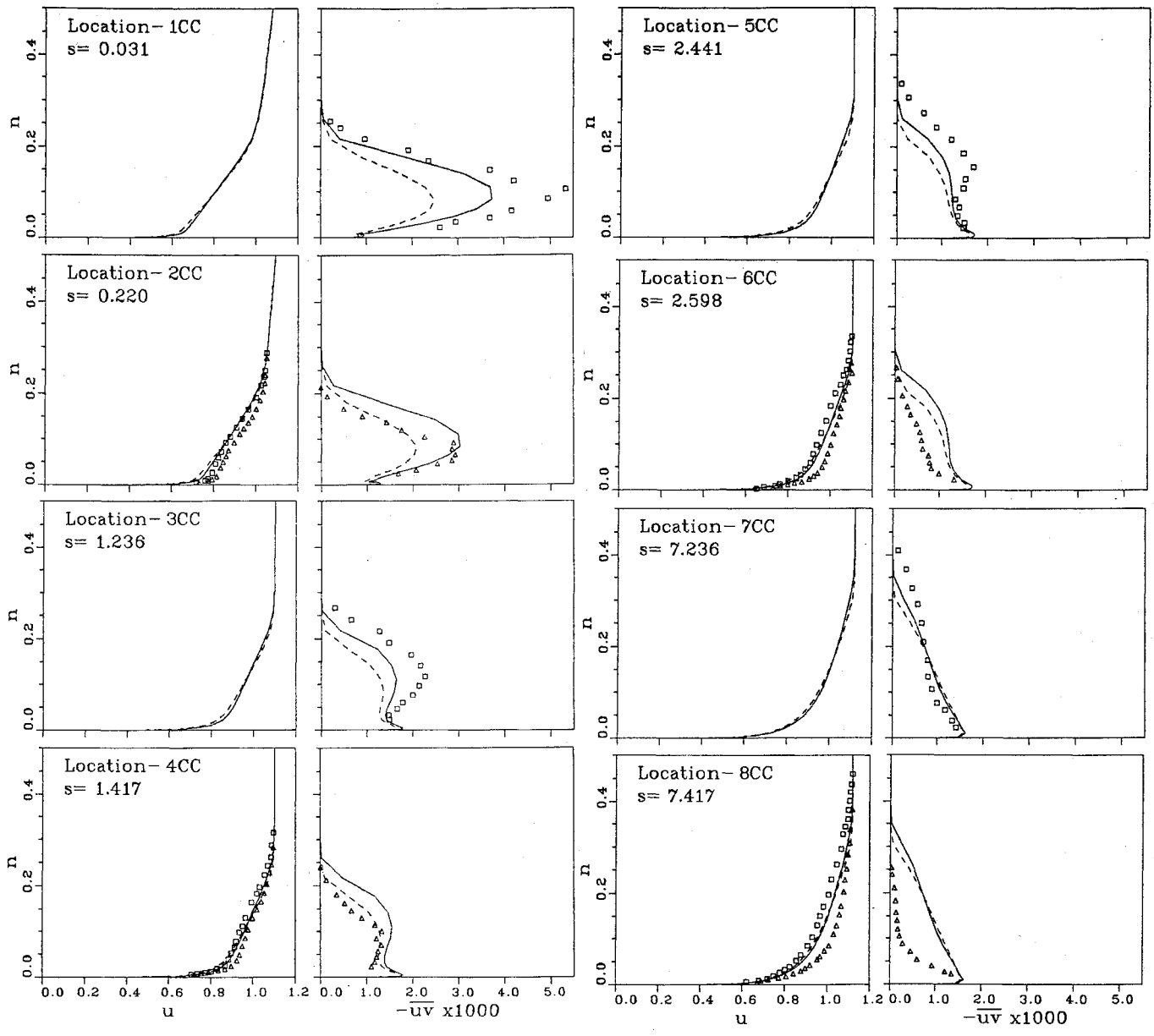

Fig. 14 Computed and measured (symbols) velocity and Reynolds shear stress profiles for the concave wall experiments (cases CC30C and CC30T) of Smits et al.[1] The variable n is the distance normal to the concave wall nondimensionalized by the duct width. Solid lines, HL model; dashed lines, standard k-ϵ model. Measurements at the point of minimum (squares) and maximum (triangles) wall shear stress.

tion. The opposite occurs at a point of minimum wall shear stress. The computed results are in fair agreement with the average flow.

The experiment of Smits et al.[1] differs from the others in that the strong curvature induces severe pressure gradients near the inlet and exit of the bend and in that measurements of the relaxation process were made in the straight recovery section, which followed the curved section. The computational domain employed a shorter upstream straight section than was used in the actual wind tunnel. The computations were performed using a 101×81 grid.

Figure 11 shows the pressure and skin-friction coefficients computed using the HL model. The overall pressure distribution agrees satisfactorily with the data. On the convex-wall side the computed skin friction is overpredicted in the region immediately downstream of the curve by as much as 30%, although, rather surprisingly, the predictions on the concave-wall side compare well with the spanwise minimum values. Figure 11 also shows the convex wall shear stress computed by Gibson et al.[3] using a Reynolds-stress model and a boundary-layer calculation method. The two computations are in substantial agreement, except immediately downstream of the curve. The differences are most likely caused by the pressure in the present method being computed, and not specified, as in the boundary-layer calculations. The wall shear stresses predicted by the HL and standard models are compared in Fig. 12. The HL model yields improved results and seems to be more effective in the present case than in the previous one.

The velocity and Reynolds stress profiles shown in Fig. 13 display the same trends as those observed in the previous cases. The degree to which the Reynolds stress is overpredicted is displayed in the results at location 2. The data indicate that the strong stabilizing curvature has destroyed the Reynolds stress in the outer part of the boundary layer, but the computations do not reproduce this behavior. As expected, the agreement between the measurements and calculations improves as the boundary layer returns to a flat-surface structure in the recovery section.

Figure 14 shows the computed and measured velocity and Reynolds stress profiles at several stations along the concave wall. The measurements clearly show the influence of the Taylor-Goertler vortices. The vortex system is still present at location 8CC, more than 7 duct widths, or 31 boundary-layer thicknesses, downstream of the bend. Here again, the com-

puted velocity and Reynolds stress profiles are representative of the spanwise average value of the measurements. The underprediction of the velocity at location 2CC probably is due to the underprediction of the favorable pressure gradient at the exit of the curved section, rather than being an inaccurate prediction of the Reynolds shear stress.

It should be noted that the experimental measurements on the convex and concave walls may be affected by streamline convergence and divergence, respectively, initiated by the radial pressure gradients acting on the sidewall boundary layers. Such effects are more likely to be present in the Muck et al.[7] and Smits et al.[1] studies, because of the small aspect ratios (6.0) of their wind tunnels. The aspect ratio of the duct used by Eskinazi and Yeh[6] was much larger (15.5), and presumably the secondary-flow effects were smaller. These effects might account for the large deviations in the wall shear stress observed in the mildly curved flow of Muck et al., especially considering that the friction coefficient was predicted rather well on the convex wall for the strong curvature case of Eskinazi and Yeh.

Conclusions

The general numerical method developed in Ref. 5 for solving the Reynolds-averaged Navier-Stokes equations has been applied to several flows in which pressure-gradient and surface-curvature effects are important. The capability of the method to consider a wide range of geometries was illustrated by the curved-duct computations. In each case the main features of the flow (e.g. the pressure distributions and velocity profiles) were reproduced consistently with reasonable accuracy.

The calculations for the fully developed curved-duct flow and the boundary layers developing in curved ducts each show that the standard k-ϵ model as well as the modification of it proposed by Hanjalic and Launder (the HL model) tend to overpredict the turbulent shear stress near a convex wall and likewise underpredict it near a concave wall. The HL model appears to be more effective in reproducing the destabilizing influence of concave curvature. However, the poor agreement that persists near the concave wall is caused in part by the present two-dimensional computations not explicitly accounting for the significant three-dimensional flow effects resulting from the presence of Taylor-Goertler vortices. The model also calculated with reasonable accuracy the recovery of turbulent boundary layers on a flat surface following exposure to curvature corresponding to the experiments of Smits et al.,[1] although the turbulent shear stress suffered from the deficiencies noted earlier. It is significant that in this case the present method yields results similar in quality to those obtained using more complex turbulence models.

The deficiencies observed in the present computations using the complete Reynolds equations have also been noted in several previous studies based on the solution of the boundary-layer equations, with and without higher-order terms and with a variety of turbulence models. In fact, the results of these previous studies and the present one are so similar that one is led to conclude that the approximations made in the boundary-layer equations are not entirely responsible for the lack of agreement between the computations and measurements. It is more likely that inadequacies in the turbulence models, the effects of Taylor-Goertler vortices, and the possible, yet unknown, influence of secondary flows in the experiments are largely responsible for the disagreements. The HL model, with its curvature-inspired modification, represents an improvement on the standard k-ϵ model, but it is not entirely successful.

In closing, we suggest that future experimental and computational investigations that seek to further clarify the effects of surface curvature on turbulent flow should include the effects of longitudinal and normal pressure gradients and not be restricted to boundary-layer equations and concepts. This would facilitate the development and testing of general computational methods for complex turbulent flows.

Acknowledgments

This research was supported by the Office of Naval Research under the Accelerated Research Initiative (Special Focus) Program in Ship Hydrodynamics, Contract N00014-83-K-0136. The Battelle/Marine Sciences Laboratory is part of the Pacific Northwest Laboratory, which is operated for the U.S. Department of Energy by Battelle Memorial Institute under Contract DE-AC06-76RLO 1830.

References

[1]Smits, A. J., Young, S. T. B., and Bradshaw, P., "The Effect of Short Regions of High Surface Curvature on Turbulent Boundary Layers," *Journal of Fluid Mechanics*, Vol. 94, Pt. 2, 1979, pp. 209-242.

[2]Gillis, J. C., and Johnston, J. P., "Turbulent Boundary Layer Flow and Structure on a Convex Wall and its Redevelopment on a Flat Wall," *Journal of Fluid Mechanics*, Vol. 135, 1983, pp. 123-153.

[3]Gibson, M. M., Jones, W. P., and Younis, B. A., "Calculation of Turbulent Boundary Layers on Curved Surfaces," *Physics of Fluids*, Vol. 24, No. 3, 1981, pp. 386-395.

[4]Chen, H. C., and Patel, V. C., "Near-Wall Turbulence Models for Complex Flows Including Separation," *AIAA Journal*, Vol. 26, No. 6, 1988, pp. 641-648.

[5]Richmond, M. C., "Surface Curvature and Pressure Gradient Effects on Turbulent Flow: An Assessment Based on Numerical Solution of the Reynolds Equations," PhD Dissertation, Univ. of Iowa, Iowa City, IA, 1987.

[6]Eskinazi, S., and Yeh, H., "An Investigation on Fully Developed Turbulent Flows in a Curved Channel," *Journal of the Aeronautical Sciences*, Vol. 23, Jan. 1956, pp. 23-34.

[7]Muck, K. C., Hoffmann, P. H., and Bradshaw, P., "The Effect of Convex Surface Curvature on Turbulent Boundary Layers," *Journal of Fluid Mechanics*, Vol. 161, 1985, pp. 347-369.

[8]Richmond, M. C., Chen, H. C., and Patel, V. C., "Equations of Laminar and Turbulent Flows in General Curvilinear Coordinates," Iowa Inst. of Hydraulic Research, Univ. of Iowa, Iowa City, IA, IIHR Rept. 300, 1986.

[9]Patel, V. C., and Richmond, M. C., "Pressure Gradient and Surface Curvature Effects in Turbulent Boundary Layers," AIAA Paper 87-1301, June 1987.

[10]Kline, S. J., Cantwell, B. J., and Lilly, G. M., (eds.), *Proceedings of the 1980-81 AFOSR-HTTM-Stanford Conference on Complex Turbulent Flows*, Vol. 1-3, Department of Mechanical Engineering, Stanford Univ., Stanford, CA, 1982.

[11]Rodi, W., and Scheuerer, G., "Calculation of Curved Shear Layers with Two-Equation Turbulence Models," *Physics of Fluids*, Vol. 26, 1983, pp. 1422-1436.

[12]Chen, C. J., "The Finite-Analytic Method," Vols. 1-7, Iowa Inst. of Hydraulic Research, Univ. of Iowa, Iowa City, IA, IIHR Rept. 232, 1980-1986.

[13]Patankar, S. V., *Numerical Heat Transfer and Fluid Flow*, McGraw-Hill, New York, 1980.

[14]Chen, H. C., and Patel, V. C., "Calculation of Trailing Edge, Stern, and Wake Flows by a Time Marching Solution of the Partially-Parabolic Equations," Iowa Inst. of Hydraulic Research, Univ. of Iowa, Iowa City, IA, IIHR Rept. 285, 1985.

[15]Hunt, I. A., and Joubert, P. N., "Effects of Small Streamline Curvature on Turbulent Duct Flow," *Journal of Fluid Mechanics*, Vol. 91, 1979, pp. 633-659.

[16]Moser, R. D., and Moin, P., "Effects of Curvature in Wall-Bounded Turbulent Flows," *Journal of Fluid Mechanics*, Vol. 175, 1987, pp. 479-510.

[17]Pourahmadi, F., and Humphrey, J. A. C., "Prediction of Curved Channel Flow with an Extended k-ϵ Model of Turbulence," *AIAA Journal*, Vol. 21, No. 1, 1983, pp. 1365-1373.

[18]Hoffmann, P. H., Muck, K. C., and Bradshaw, P., "The Effect of Concave Surface Curvature on Turbulent Boundary Layers," *Journal of Fluid Mechanics*, Vol. 161, 1985, pp. 371-403.

[19]Hoffmann, P. H., and Bradshaw, P., "Turbulent Boundary Layers on Surfaces of Mild Longitudinal Curvature," Dept. of Aeronautics, Imperial College, London, IC Aero. Rept. 78-04, 1978.